

# Poly(lactic acid)-Based Biocomposites Reinforced with Kenaf Fibers

Maurizio Avella,<sup>1</sup> Gordana Bogoeva-Gaceva,<sup>2</sup> Aleksandra Bužarovska,<sup>2</sup> Maria Emanuela Errico,<sup>1</sup> Gennaro Gentile,<sup>1</sup> Anita Grozdanov<sup>2</sup>

<sup>1</sup>*Institute of Chemistry and Technology of Polymers, National Research Council, Via Campi Flegrei Comprensorio Olivetti, 80078 Pozzuoli (NA), Italy*

<sup>2</sup>*Faculty of Technology and Metallurgy, University Sts. Cyril and Methodius, R. Bošković 16, 1000 Skopje, Republic of Macedonia*

Received 13 June 2007; accepted 29 December 2007

DOI 10.1002/app.28004

Published online 6 March 2008 in Wiley InterScience (www.interscience.wiley.com).

**ABSTRACT:** Biodegradable thermoplastic-based composites reinforced with kenaf fibers were prepared and characterized. Poly(lactic acid) (PLA) was selected as polymeric matrix. To improve PLA/fibers adhesion, low amount of a proper reactive coupling agent, obtained by grafting maleic anhydride onto PLA, was added during matrix/fibers melt mixing. Compared with uncompatibilized composites,

this compatibilization strategy induces a strong interfacial adhesion and a pronounced improvement of the mechanical properties. © 2008 Wiley Periodicals, Inc. *J Appl Polym Sci* 108: 3542–3551, 2008

**Key words:** composites; compatibility; mechanical properties; biodegradable

## INTRODUCTION

In the recent years, the use of renewable resources for the preparation of polymer-based materials has attracted a growing attention because of the increasing demand of environmental friendly materials.<sup>1,2</sup> Sustainability, eco-efficiency, and green chemistry are the guidelines to develop the next generation of materials. Biodegradable materials based on annually renewable agricultural and biomass feedstock can be competitive with products based on petroleum feedstock. Furthermore, composites based on biodegradable plastics and natural fibers (biocomposites) can be considered an excellent alternative to composites based on nonbiodegradable thermoplastics and reinforced with synthetic fibers, such as glass fibers. For example, the development of wholly biodegradable plastics can play a fundamental role in helping to solve the waste disposal problems.<sup>3</sup>

Among biodegradable plastics, poly(lactic acid) (PLA) is a very interesting material. It is a degradable thermoplastic polymer with excellent mechanical properties and is produced on a large scale from fermentation of corn starch to lactic acid and subsequent chemical polymerization. Pure PLA can degrade to carbon dioxide, water, and methane in the environment over a period of several months to 2 years, compared to other petroleum plastics needing very longer periods.<sup>4,5</sup>

On the other hand, it is well known that the fiber reinforcement is a viable method to improve the mechanical properties of biodegradable plastics and to reduce the overall costs of the prepared materials.<sup>6</sup> For this purpose, natural fibers have many advantages compared to synthetic fibers, for example, low weight, and they are recyclable and biodegradable. They are also renewable and have relatively high strength and stiffness and cause no skin irritations.<sup>7–13</sup>

The manufacturing methods of natural fiber thermoplastic composites have been improved through the optimization of lay-up/press molding (film stacking method), pultrusion, extrusion, and injection-molding methods.<sup>14,15</sup> Among lignocellulosic fibers, kenaf is attracting special attention due to its good mechanical properties (comparable to jute, sisal, and flax) and to its increasing cultivation in many developing and developed countries.<sup>16</sup> Kenaf has been already tested as natural reinforcement for polyolefins, but there is an even growing interest on the preparation of biocomposites.<sup>17,18</sup> Among these, interesting results have been reported for PLA/kenaf

Correspondence to: M. Avella (mave@ictp.cnr.it).

Contract grant sponsor: European Commission in the Sixth Framework Programme; contract grant number: FP6-2002-INCO-WBC-1.

Contract grant sponsor: Specific Measures in support of International Cooperation with Western Balkans Countries, Specific Targeted Research or Innovation Project; contract grant number: 509185.

Contract grant sponsor: ECO-PCCM—Eco-Houses Based on Eco-Friendly Polymer Composite Construction Materials.

*Journal of Applied Polymer Science*, Vol. 108, 3542–3551 (2008)  
© 2008 Wiley Periodicals, Inc.

composites.<sup>19,20</sup> In fact, improvements of PLA properties such as heat resistance, mechanical performance, and moldability have been obtained through the addition of kenaf fibers.<sup>19</sup> Nevertheless, these studies do not refer to any compatibilization strategy, unless the polymeric and the fibrous phase show different surface chemistry: lignocellulosic fibers are hydrophilic, whereas PLA is hydrophobic. Therefore, compatibilization strategies should be considered to optimize the effects of the reinforcement phase.<sup>21</sup>

In a previous work, we have prepared and characterized poly(3-hydroxybutyrate-co-3-hydroxyvalerate) (PHBV)-based biocomposites reinforced with kenaf fibers, and we have evaluated the effects of a compatibilization on the performances of these composites.<sup>22</sup> The main goal of this work was the preparation and the characterization of new PLA-based composites reinforced with kenaf fibers with particular attention to the promotion of a reactive interface between the thermoplastic matrix and the lignocellulosic filler by using a compatibilizer, following the effective strategy evidenced from the earlier work with PHBV/kenaf composites. Therefore, the influence of the improved interfacial adhesion on the final composite properties was deeply investigated. As concerning the compatibilization strategy, a proper coupling agent (CA) was synthesized by grafting maleic anhydride (MA) onto PLA backbone. Then, the composites were prepared by reactive blending, and their morphological, thermal, and mechanical properties were investigated. The influence of the CA on the final properties was studied by comparing the uncompatibilized and compatibilized composite properties.

## EXPERIMENTAL

### Materials

Kenaf fibers, average length 5.1 mm and average diameter 21  $\mu\text{m}$ , were kindly supplied by Kenaf Eco Fibers Italia S.p.A. (Guastalla-Italy) and dried at 95°C for 24 h before their use for the preparation of composites. PLA was supplied by Biomer (Krailling-Germany). MA, dibenzoylperoxide (DBPO), chloroform, methyl alcohol (MeOH), tetrahydrofuran (THF), hydrochloric acid (HCl) and morpholine (Sigma-Aldrich reagent products, Steinheim-Germany) were used as received.

### Coupling agent preparation

About 48.5 g (47.5 g; 46.5 g) of PLA were mixed for 5 min in an internal mixer (Brabender-like apparatus, Rheocord EC of HAAKE Inc., New Jersey, USA) at 170°C, then 1.5 g (2.5 g; 3.5 g) of MA and 0.75 g of DBPO were added. The mixture was blended at

180°C for further 5 min, increasing progressively the mixing rate up to 32 rpm. Finally, the obtained material was dried under vacuum at 100°C to remove the unreacted MA. The obtained CA was coded as CA3 (CA5; CA7).

### PLA-based composites preparation

PLA-kenaf composites were prepared by melt mixing in an internal mixer (Brabender-like apparatus, Rheocord EC of HAAKE, NJ). Two kinds of composites were prepared through the following procedures. Uncompatibilized composites were obtained by mixing 40 g (35 g) of PLA at 180°C for 3 min. Then, 10 g (15 g) of kenaf fibers, previously dried at 95°C for 24 h under vacuum, were added, and the mixture was blended at 180°C for further 10 min, increasing progressively the mixing speed up to 32 rpm. Corresponding sample is coded as PLA/K 80/20 (PLA/K 70/30). Compatibilized PLA-kenaf composites were prepared as follows: 37.5 g (32.5 g) of PLA and 2.5 g of CA3 were mixed in the Brabender-like apparatus for 5 min. Thereafter, 10 g (15 g) of dry kenaf fibers were added, and the mixture was blended at 180°C for further 10 min, increasing progressively the mixing rate up to 32 rpm. Corresponding sample is coded as PLA/CA/K 75/5/20 (PLA/CA/K 65/5/30).

### Preparation of compression-molded sheets

Neat PLA and PLA-based composites were compression molded in a heated press at 180°C for 5 min without any applied pressure. After this period, a pressure of 100 bar was applied for 5 min, then the press plates, equipped with cooling coils, were quickly cooled to room temperature by cold water. Finally, the pressure was released, and the mold was removed from the plates. Films (thickness about 100  $\mu\text{m}$ ) and sheets (thickness about 3.5 mm) were obtained.

### Techniques

#### Fourier-transformed infrared analysis

FTIR spectra of neat PLA and PLA grafted with different amount of MA were recorded at room temperature with a Perkin-Elmer Paragon 2000 Fourier Transform Infrared spectrometer (Wellesley, MA), using 64 scans and a resolution of 2  $\text{cm}^{-1}$ . FTIR spectra were collected on thin films (thickness about 100  $\mu\text{m}$ ) prepared by compression molding.

#### Potentiometric titration

The extent of maleation of PLA samples grafted with MA was determined by titration using a Crison

TitroMatic potentiometric titrator.<sup>23,24</sup> One gram of CA3 (CA5; CA7) was dissolved in 20 mL of THF-MeOH (5 : 1 by volume). After complete dissolution, 6.0 mL of morpholine solution (0.05N in MeOH) were added; the mixture was let to react for 10 min, and then the sample was titrated samples with 0.01N HCl. The HCl solution was titrated against a known NaOH standard. The morpholine solution was then titrated against the HCl to obtain a blank. The same procedure was carried out on neat PLA.

#### Viscometric analysis

The viscometric molecular weight ( $M_w$ ) of neat PLA, PLA processed at 180°C for 10 min, and PLA grafted with MA (CA) was determined in chloroform at 25°C by means of Cannon-Ubbelohde viscometer.  $M_w$  values were obtained by using the Mark-Houwink-Sakurada relationship.<sup>25,26</sup>

$$[\eta] = KM_w^\alpha$$

where  $K = 0.0074 \text{ mL g}^{-1}$  and  $\alpha = 0.87$ .<sup>27,28</sup>

#### Morphological analysis

The morphological analysis was performed by using scanning electron microscope, Cambridge Stereoscan microscope model 440, on cryogenically fractured surfaces of the composite samples. Before the observation, the specimens were metallized with a gold/palladium coating.

#### Thermogravimetric analysis

The thermal stability of samples was measured by means of TGA with a Perkin-Elmer Pyris Diamond Thermogravimetric/Differential Thermal Analyzer, recording the weight loss as a function of the temperature. Samples were heated from 40 to 700°C at a scanning rate of 10°C/min under nitrogen atmosphere. Degradation temperature values ( $T_d$ ) were evaluated as temperatures corresponding to the maximum rate of the weight loss.

#### Dynamic-mechanical analysis

Dynamic-mechanical data were collected at 1 Hz and at a heating rate of 3°C/min from -50 to 120°C under nitrogen flow with a Perkin-Elmer Pyris Diamond Dynamic Mechanical Analyzer. The experiments were performed in bending mode on samples 20 mm long, 14 mm wide, and 3.5 mm thick.

#### Mechanical analysis

The flexural strength and the flexural modulus were measured in a three-point bending mode using an

Instron machine (model 5564), at a cross-head speed of 1 mm/min and at room temperature. Test specimens were 3.5 mm thick, 6.0 mm wide, and 60 mm long. The test span was 48.0 mm. For each sample, 10 specimens were tested, and the average values of the flexural strength and modulus were calculated.

Fracture tests were carried out with a Charpy Ceast Resil Impactor equipped with a DAS 4000 Acquisition System at an impact speed of 1 m/s. Samples with a notch depth to width ratio of 0.3 and a span length of 48.0 mm, 6.0 mm wide, 3.5 mm thick, and 60 mm long were fractured at room temperature (ASTM D256). The relative curves of energy and load were recorded. For each sample, 10 specimens were fractured, and the average values of the resilience were calculated.

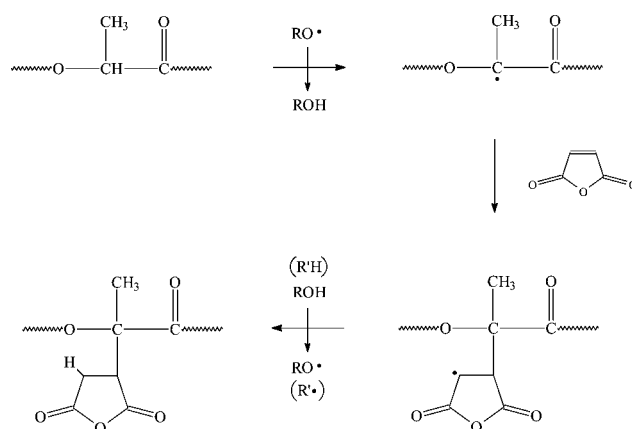
## RESULTS AND DISCUSSION

### Chemical modification of PLA

It is well known that the set up of a proper compatibilization among the phases plays a critical role to obtain high-performance multiphase systems. As a matter of fact, to promote PLA/kenaf fibers adhesion, a reactive CA was prepared. In particular, PLA backbone was modified by grafting different amount of MA through the thermal decomposition of DBPO, according to the mechanism illustrated in Scheme 1.<sup>24,29</sup> This choice allowed the reduction of the overall environmental impact of the process with respect to a chemical modification carried out in solution.<sup>30,31</sup>

### FTIR spectroscopy

The grafting reaction of MA onto PLA was monitored by FTIR analysis performed onto PLA-g-MA previously purified by removing an unreacted MA.



**Scheme 1** Reaction scheme between PLA and maleic anhydride (MA) in the presence of dibenzoylperoxide (DBPO).

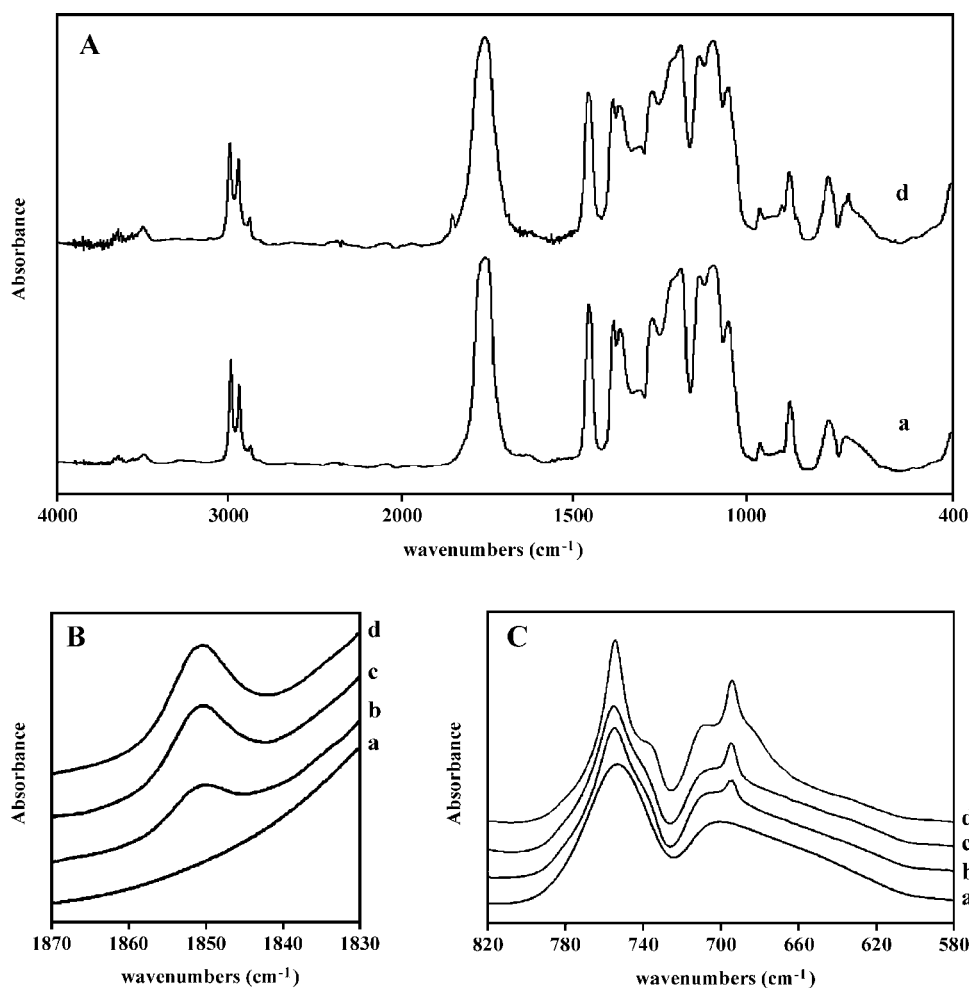


**Figure 1** FTIR spectra of (a) neat PLA; (b) PLA grafted with 3% MA (CA3); (c) PLA grafted with 5% MA (CA5); (d) PLA grafted with 7% MA (CA7).

In Figure 1, FTIR spectra of neat PLA and modified PLA are reported. In Figure 1(B,C), only the spectral regions  $1870\text{--}1830\text{ cm}^{-1}$  and  $820\text{--}580\text{ cm}^{-1}$  are reported to highlight the main differences between unmodified and modified PLA. The spectra have been normalized with respect to the absorption band centered at  $2994\text{ cm}^{-1}$  (C—H stretching of the methyl group) whose intensity is not influenced by the grafting reaction to compare the differences shown by samples grafted with different amount of MA (CA3, CA5, and CA7). As it can be observed, new absorption bands at about  $1855\text{ cm}^{-1}$  and  $695\text{ cm}^{-1}$ , whose intensities are functions of MA amount, appear in the spectra of modified PLA. These bands can be attributed to the asymmetric stretching of the MA carbonyl group and to the bending of the CH group of the anhydride ring involved into the grafting reaction, respectively, thus confirming that the foreseen reaction occurred. In Table I, the ratio between the intensities of the absorption bands centered at  $1855\text{ cm}^{-1}$  are reported for CA3, CA5, and CA7. It can be observed that

increasing the amount of MA added during the grafting reaction the relative intensity of the absorption bands centered at  $1855\text{ cm}^{-1}$  increase only up to 1.63.

#### Titration methods

To evaluate the grafting yield, the amount of MA grafted to the polymer backbone was determined by titration. Corresponding results are reported in Table I. It can be observed that increasing the amount of MA from 3 to 7% by weight for the modification of PLA, the effective content of MA grafted onto PLA backbone increases from 0.91% (CA3) to 1.51% (CA7), whereas the grafting yield decreases from 30.4% (CA3) to 21.6% (CA7). This result is supported by several papers in which it is reported that maleation of PLA by reactive blending or reactive extrusion brings to low-grafting yields.<sup>24,32</sup> Nevertheless, reactive blending and reactive extrusion are the preferred preparation methodologies for both economical and environmental factors.

**TABLE I**  
**Results of FTIR Analysis, Titration, and Viscometric Analysis Carried Out on PLA Neat, Processed, and Modified with MA**

Samples	FTIR analysis Relative intensities of the absorption bands at 1855 cm <sup>-1</sup>	Titration		Viscometric analysis <i>M<sub>w</sub></i> (Da)
		Amount of MA grafted onto PLA (% by weight)	MA grafting yield (%)	
PLA neat	–	–	–	118,000
PLA processed	–	–	–	112,000
CA3	1.00	0.91	30.4	106,000
CA5	1.38	1.23	24.5	91,000
CA7	1.63	1.51	21.6	83,000

### Viscometric analysis

The effects of the grafting reaction conditions on the eventual PLA degradation were also evaluated. Therefore, neat PLA, PLA processed at 180°C for 10 min in the presence of 1.5 wt % DBPO, and PLA grafted with different amount of MA (CA3, CA5, and CA7) were undergone viscometric analysis. In Table I, corresponding results are reported. As it is shown, the process conditions are not responsible for a significant decrease of the PLA molecular weight. This result confirms that DBPO does not induce drastic random scission reactions of the polyester chains in the selected experimental conditions. On the other hand, as concerns the grafting reactions, PLA degradation was observed as a function of the MA content. This finding can be explained taking into account that higher the MA amount, higher radical molecule concentration that could induce macromolecular scission, thus significantly reducing the PLA molecular weight, as shown in the simplified mechanism reported in Scheme 2.<sup>24</sup> This phenomenon is particularly evident for CA5 and CA7.

As a matter of fact, on the basis of the results obtained by the evaluation of both maleation yielding and PLA degradation occurred on PLA modified with different amount of MA, CA3 was selected as the most suitable reactive CA for the preparation of compatibilized composites.

### Compatibilized PLA/kenaf composites

PLA-based composites were prepared by a proper *in situ* reactive compatibilization. This preparation strategy consisted into the addition of low amount of PLA-g-MA (reactive CA) to the composite components. This CA is constituted by PLA segments identical to the polymeric matrix, and by MA groups grafted onto PLA segments, which result reactive with respect to hydroxyl groups present onto fiber surface. In this way, interactions between hydroxyl and MA groups, generating during the mixing, are responsible for *in situ* formed grafted species that

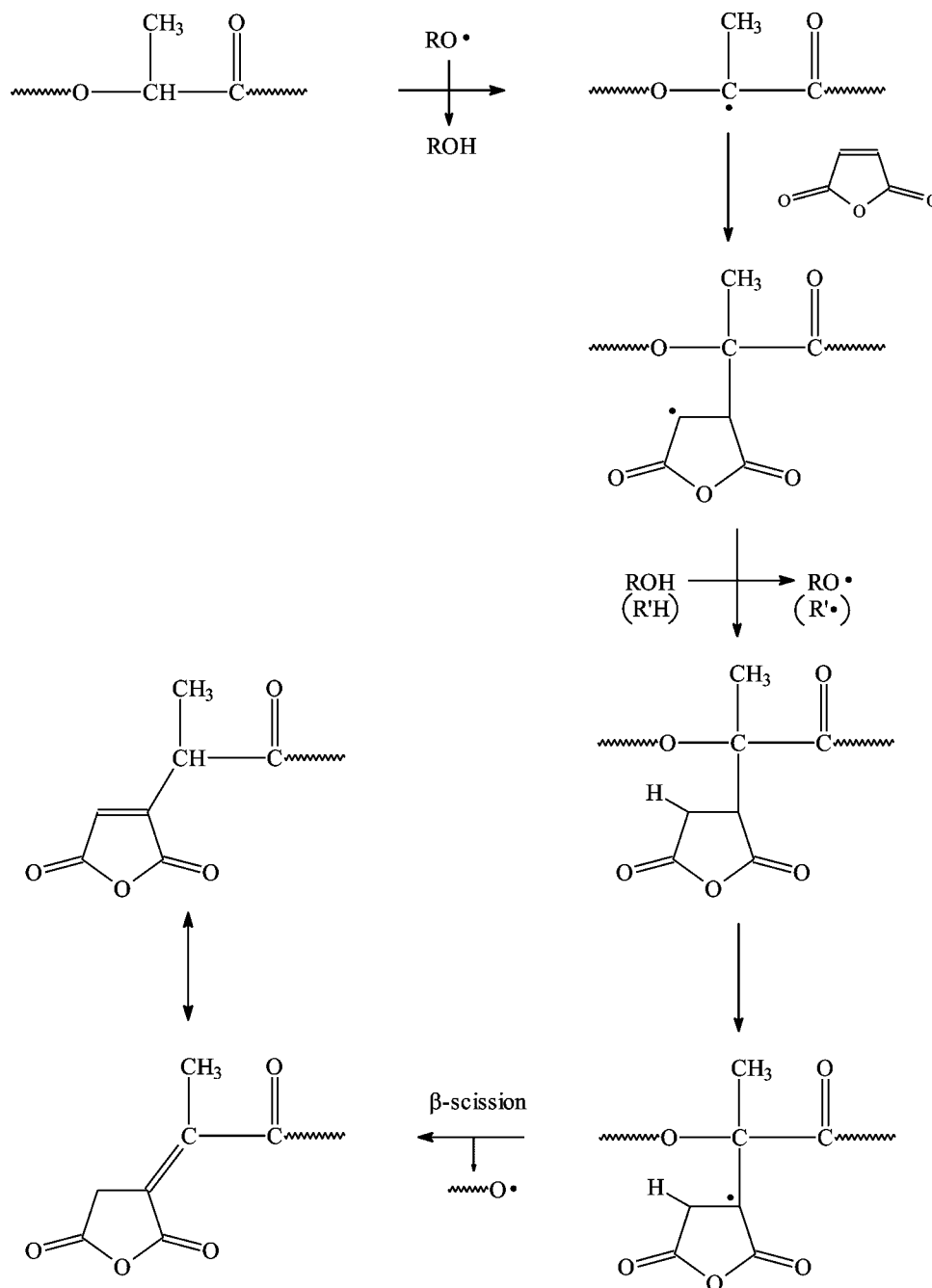
can act as an effective compatibilizer for the PLA/fiber composite components.<sup>33–35</sup>

A compatibilization strategy based on PLA modification was preferred to the chemical modification of cellulose fibers. The latter is usually performed by using dicarboxyl acid anhydrides such as succinic (SA) and maleic (MA) anhydrides to esterify cellulose fibers, as illustrated elsewhere.<sup>36</sup> Nevertheless, it has been widely pointed out that exchange reactions may occur during the melt mixing of polyesters, in the presence of species containing reactive end groups, such as hydroxyl, carboxyl, and amine groups.<sup>37,38</sup> As a matter of fact, carboxyl end groups bonded to cellulose fibers could attack the inner ester groups of PLA, yielding random scission reactions. As a consequence, a drastic decrease of PLA molecular weight could occur with a decrease of mechanical strength, chemical, and thermal resistance of the polymer.<sup>39–41</sup>

To evaluate the influence of the reactive compatibilization on the morphology and final properties of the composites, uncompatibilized materials were also prepared.

### Morphological analysis

The morphological analysis was performed on cryogenically fractured surfaces of uncompatibilized and compatibilized materials, thus allowing to evaluate not only the fiber dispersion but also the fiber/matrix adhesion level after an applied external load. As an example, in Figure 2, the micrographs of composites containing the highest amount of kenaf fibers (30% by weight) are reported. As concerns PLA/K 70/30 composite [see Fig. 2(A)], kenaf fibers appear not wholly embedded into PLA matrix. Moreover, the fibers are strongly damaged, and some debonding phenomena can be evidenced as a result of the cryogenic fracture, thus indicating a poor fiber-polymer adhesion. Instead, as it can be observed from Figure 2(B), a significant enhancement of the adhesion level between the fibers and the matrix can be remarked for the compatibilized PLA/CA/K 65/5/30



**Scheme 2**  $\beta$ -Scission mechanism of PLA during grafting with maleic anhydride (MA) in presence of dibenzoylperoxide (DBPO).

composite. In fact, the fibers are well welded into PLA and the absence of voids indicates that no debonding phenomena occur. This result permits to assess that the reactive compatibilization allows a significant improvement of the fiber-polymer interfacial adhesion.

#### Thermal and thermogravimetric analysis

Table II resumes thermal parameters (glass transition and degradation temperature) of neat PLA and PLA-

based composites collected by DMA and TGA analyses. As concerns the glass transition temperature ( $T_g$ ), a slight increase of  $T_g$  values was recorded for compatibilized PLA-based composites. This result can be justified considering that the presence of the reactive CA promotes a good fiber/matrix interfacial adhesion responsible for a reduced chain mobility of the polymeric matrix.

The thermal stability of kenaf, neat PLA, and PLA-based composites was investigated in terms of weight loss as a function of temperature by thermo-

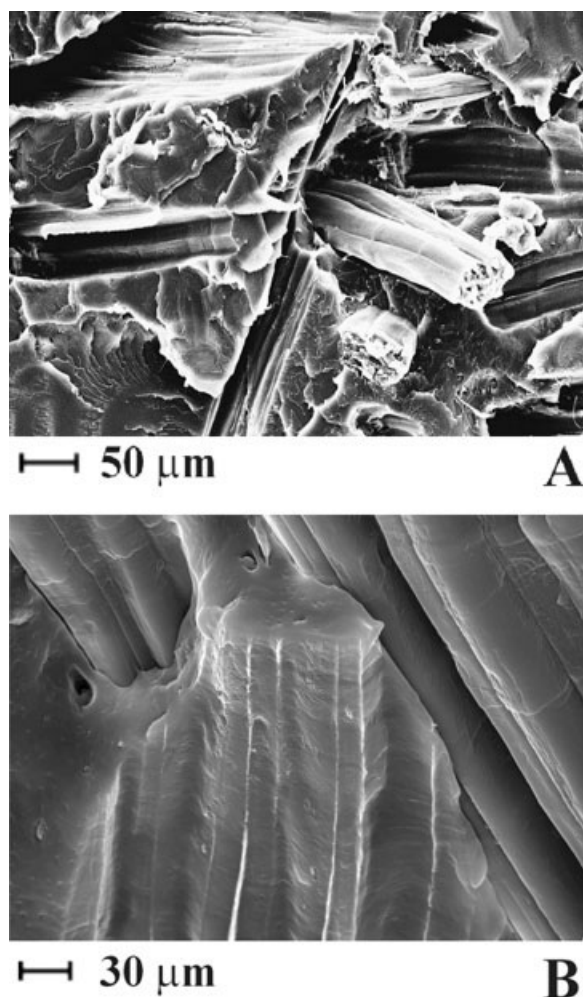


**Figure 2** SEM micrographs of (A) uncompatibilized PLA/K 70/30 composite; (B) compatibilized PLA/CA/K 65/5/30 composite.

gravimetric analysis carried out in nitrogen flow. In Table II, the degradation temperature values ( $T_d$ ), calculated as the maximum of the degradation rate, and the residual weight at 500°C are reported. Moreover, in Figure 3, thermogravimetric traces are reported for PLA and PLA/kenaf composites. It can be observed that for both kenaf and PLA, the ther-

**TABLE II**  
Glass Transition Temperatures ( $T_g$ ), Degradation Temperature ( $T_d$ ), and Residual Weight at 500°C of Neat PLA and PLA-Based Composites

Codes	$T_g$ (°C)	$T_d$ (°C)	Weight residual at 500°C (%)
PLA neat	58	365	0.9
Kenaf	–	348	17.2
PLA/K 80/20	57	355	5.1
PLA/K 70/30	58	354	7.2
PLA/CA/K 75/5/20	62	352	5.1
PLA/CA/K 65/5/30	62	351	7.2

mal degradation occurs in a single step, whose maximum rates are centered at 348 and 365°C, respectively. In the case of PLA-based composites, degradation of matrix and fibers appear as overlapped phenomena, due to the comparable degradation temperatures of kenaf and PLA. Moreover, the presence of the reactive CA does not affect the thermal degradation process. In fact, the weight residual curves of the compatibilized and uncompatibilized materials containing the same amount of fibers are similar. The maximum rate of this overall degradation process is centered at 351–354°C, and it does not seem to be a function of the fiber content and the compatibilization.

Finally, as concerning the residual weight at 500°C, it can be remarked that kenaf shows a very high residual weight, about 17%, in agreement with data reported in literature for cellulose fibers.<sup>42</sup> As a consequence, the residual weight at 500°C is higher for composites with the highest kenaf amount (PLA/K 70/30 and PLA/CA/K 65/5/30) with respect to that recorded for composites containing 20% by

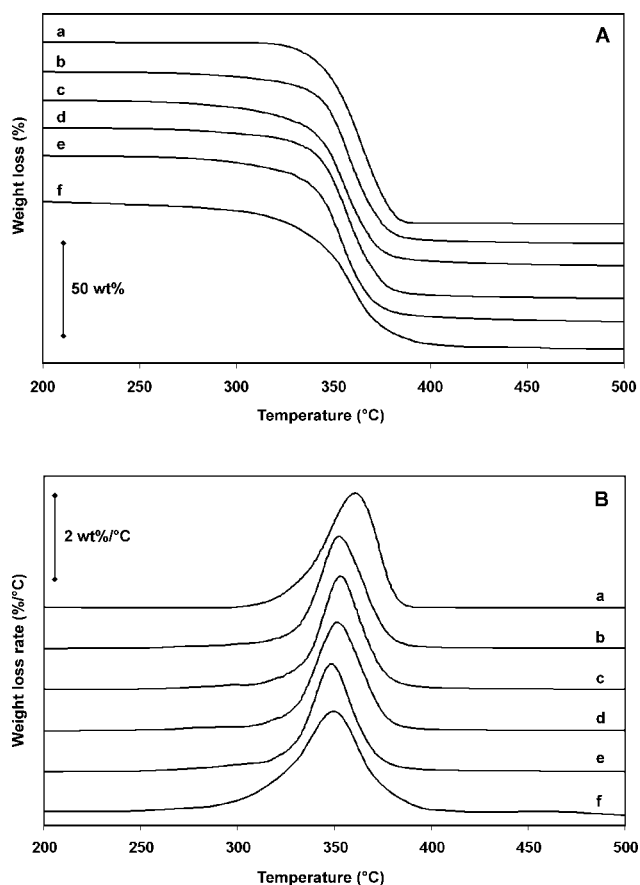


**Figure 3** Results of the thermogravimetric analysis under  $N_2$  flow: (A) weight loss and (B) weight loss rate for the samples: (a) neat PLA; (b) PLA/K 80/20; (c) PLA/K 70/30; (d) PLA/CA/K 75/5/20; (e) PLA/CA/K 65/5/30; (f) kenaf fibers.

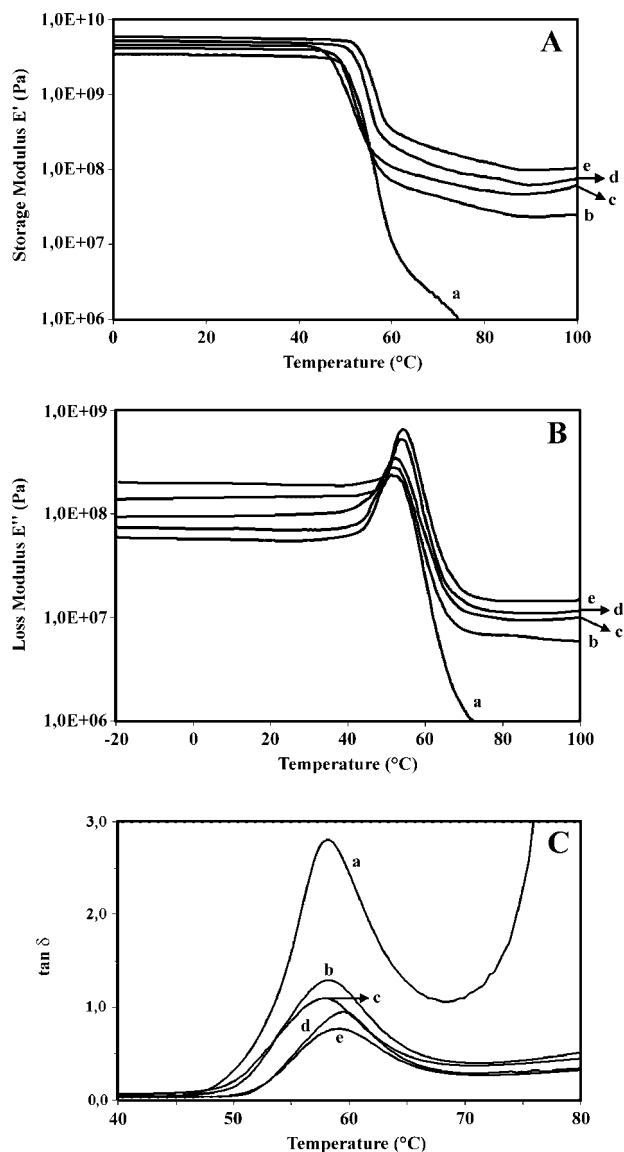


**Figure 4** Results of the DMA analysis: (A) storage modulus  $E'$ , (B) loss modulus  $E''$ , and (C)  $\tan \delta$  for the samples: (a) neat PLA; (b) PLA/K 80/20; (c) PLA/K 70/30; (d) PLA/CA/K 75/5/20; (e) PLA/CA/K 65/5/30.

weight of kenaf fibers (PLA/K 80/20 and PLA/CA/K 75/5/30).

### Mechanical and thermomechanical analysis

DMA results are illustrated in Figure 4. It can be observed that both the storage modulus ( $E'$ ) [Fig. 4(A)] and the loss modulus ( $E''$ ) [Fig. 4(B)] increase with the fiber content. Furthermore, it can be remarked that the highest storage and loss modulus improvements were recorded for compatibilized composites and that the presence of kenaf fibers drastically reduces the extent of  $E'$  and  $E''$  decrease with respect to neat PLA.

In Figure 4(C),  $\tan \delta$  curves are reported. As it is possible to observe a pronounced decrease of the

maximum value of the  $\tan \delta$  as a function of the fiber content and reactive compatibilization was obtained. Moreover, the temperature relative to the maximum of  $\tan \delta$ , which corresponds to the glass transition temperature, is also influenced by reactive compatibilization procedure, as discussed earlier and reported in Table II.

The reduction of the maximum value of the  $\tan \delta$  is correlated to the increase of the storage and loss modulus, thus suggesting an improvement of the PLA-based composites stiffness that is a function of fiber content and overall of the reactive compatibilization. In fact, the compatibilization procedure is able to promote better fiber-matrix adhesion with respect the uncompatibilized materials, in agreement with the results obtained by morphological analysis.

To confirm this assumption, the adhesion parameter  $A$  of the fiber-matrix interface was also evaluated.<sup>43,44</sup> The parameter  $A$  is defined by the following equation:<sup>45</sup>

$$A = \frac{1}{1 - V_F} \times \frac{\tan \delta_C(T)}{\tan \delta_M(T)} - 1$$

where  $V_F$  is the volume fraction of the filler in the composite, and  $\tan \delta_C(T)$  and  $\tan \delta_M(T)$  are the values of  $\tan \delta$ , measured at the temperature  $T$ , of the composite and the pure matrix, respectively. It is to be remarked that the adhesion parameter  $A$  is inversely correlated with the adhesion level between the composite components, that is, to lower  $A$ , higher fiber-matrix interactions correspond. The adhesion parameter  $A$  is graphed versus temperature in Figure 5. As it can be observed, the adhesion level is a function of the fiber content and of the reactive compatibilization. In fact, for both uncompatibilized (curves a and b) and compatibilized (curves c and d) composites, lower kenaf contents induces stronger interactions between matrix and fibers. Moreover, the adhesion parameter curves of compatibilized samples lay below those of the uncompatibilized

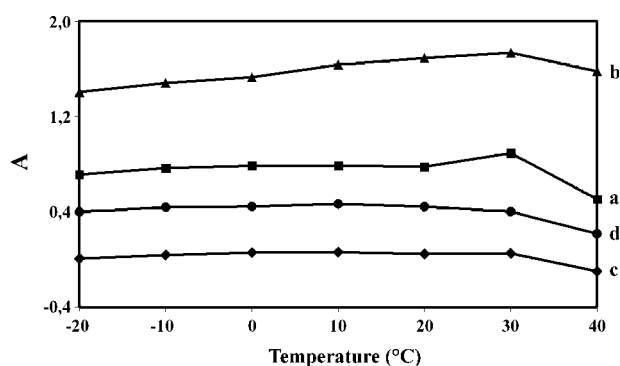


**Figure 5** Adhesion parameter  $A$  for the samples: (a) PLA/K 80/20; (b) PLA/K 70/30; (c) PLA/CA/K 75/5/20; (d) PLA/CA/K 65/5/30.



**TABLE III**  
**Mechanical Analysis Results**

Sample	Impact analysis		Flexural analysis	
	Resilience (kJ/m <sup>2</sup> )	Stress at maximum load (MPa)	Modulus (MPa)	
PLA neat	1.20 ± 0.05	30.9 ± 0.2	3550 ± 50	
PLA/K 80/20	1.58 ± 0.07	32.4 ± 0.4	4630 ± 60	
PLA/K 70/30	2.24 ± 0.09	36.7 ± 0.4	5230 ± 40	
PLA/CA/K 75/5/20	2.70 ± 0.12	37.8 ± 0.9	5200 ± 60	
PLA/CA/K 65/5/30	3.46 ± 0.13	46.7 ± 0.8	5490 ± 60	

composites evidencing a stronger interfacial adhesion between fibers and matrix. This trend further confirms that the reactive compatibilization is an effective strategy to promote strong fiber-matrix interactions.

Mechanical analysis of neat PLA and PLA-based composites was performed at low (flexural) and high (impact) deformation rate to evaluate the influence of the fiber content and the compatibilization process on the stiffness and the toughness of prepared composites. Main mechanical parameters are reported in Table III. Significant improvements of the modulus (*E*) up to 55% were recorded as a function of kenaf fiber content and interfacial adhesion strength for PLA-based composites. In fact, kenaf fibers act as rigid filler responsible for the increasing of the stiffness of polymeric matrix. Moreover, the extent of the modulus improvement is also correlated to the fiber/matrix interfacial adhesion justifying the highest *E* values obtained in presence of the reactive CA.

As concerns the impact properties, previous studies reported in literature already discussed the increase of PLA toughness by addition of kenaf fibers. However, this result is also attributable to the presence of a flexibilizing agent.<sup>20</sup> As shown in Table III, in this work, the resilience of neat PLA was increased of 32 and 87% for uncompatibilized composites containing 20% (PLA/K 80/20) and 30% (PLA/K 70/20) by weight of kenaf fibers, respectively. As concerns, the compatibilized materials, still higher increases, up to about 190%, were obtained by the addition of kenaf fibers. The improvement of the discussed mechanical parameters can be explained considering that kenaf fibers act as reinforcement phase, representing critical area in which the applied load is concentrated. The extent of these phenomena is a function of the matrix/fibers interfacial adhesion strength, confirming that the compatibilization process is an effective strategy to increase performances of polymer-based composites.<sup>22</sup>

## CONCLUSIONS

A new class of biodegradable PLA-based composites reinforced with kenaf fibers was prepared and char-

acterized. The approach based on the preparation of a proper reactive CA has demonstrated that it is possible to improve the interfacial adhesion between the polyester and the kenaf fibers, strongly enhancing the final properties of composites. In particular, main results can be summarized as follows.

Compatibilized PLA/kenaf composites show an improved adhesion between fibers and matrix, as confirmed both by morphological analysis and by the evaluation of the adhesion parameter.

Thermogravimetric analysis shows that the kenaf fibers and the reactive compatibilization do not significantly influence the thermal stability of PLA.

The reactive compatibilization procedure induces significant improvements of flexural and impact properties in comparison with uncompatibilized PLA-based composites.

## References

- Mohanty, A. K.; Misra, M.; Drzal, L. T. *J Polym Environ* 2002, 10, 19.
- Mwaikambo, L. Y. In *Low Environmental Impact Polymers*; Tucker, N., Johnson, M., Eds.; Rapra Technology Limited: Shawbury, UK, 2004; pp 1-24.
- Ishiku, U. S.; Pang, K. W.; Lee, W. S.; Mohd Ishak, Z. A. *Eur Polym J* 2002, 38, 393.
- Viswas, M. G.; Aristippos, G.; Milford, A. H. *Bioresour Technol* 2001, 76, 57.
- Wang, H.; Sun, X. Z.; Seib, P. *J Appl Polym Sci* 2001, 82, 1761.
- Shibata, M.; Takachiyo, K.-I.; Ozawa, K.; Yosomiya, R.; Takeishi, H. *J Appl Polym Sci* 2002, 85, 129.
- Oksman, K.; Wallstrom, L.; Berglund, L. A.; Filho, R. D. T. *J Appl Polym Sci* 2002, 84, 2358.
- Oksman, K. *J Reinf Plast Compos* 2001, 20, 621.
- Heijenrath, R.; Peijs, T. *Adv Compos Lett* 1996, 5, 81.
- Oksman, K. *Appl Compos Mater* 2000, 7, 403.
- Oksmana, K.; Skrifvars, M.; Selinc, J. F. *Compos Sci Technol* 2003, 63, 1317.
- Avella, M.; Casale, L.; Dell'Erba, R.; Focher, B.; Martuscelli, E.; Marzetti, A. *J Appl Polym Sci* 1997, 68, 1077.
- Avella, M.; Casale, L.; Dell'Erba, R.; Martuscelli, E. *Macromol Symp* 1998, 127, 11.
- Sanadi, A. R.; Cauldfield, D. F.; Rowell, R. M. *Plast Eng* 1994, 4, 27.
- Bledzki, A. K.; Reihmane, S.; Gassan, J. *J Appl Polym Sci* 1996, 59, 1329.

16. Kaldor, A. F. *Tappi J* 1992, 10, 141.
17. Chen, H.-L.; Porter, R. S. *J Appl Polym Sci* 1994, 54, 1781.
18. Karnani, R.; Krishnan, M.; Narayan, R. *Polym Eng Sci* 1997, 37, 476.
19. Nishino, T.; Hirao, K.; Kotera, M.; Nakamae, K.; Inagaki, H. *Compos Sci Technol* 2003, 63, 1281.
20. Serizawa, S.; Inoue, K.; Iji, M. *J Appl Polym Sci* 2006, 100, 618.
21. Lee, S. G.; Choi, S.-S.; Park, W. H.; Cho, D. *Macromol Symp* 2003, 197, 89.
22. Avella, M.; Bogoeva-Gaceva, G.; Bužarovska, A.; Errico, M. E.; Gentile, G.; Grozdanov, A. *J Appl Polym Sci* 2007, 104, 3192.
23. Johnson, J. B.; Funk, G. L. Determination of carboxylic acid anhydrides by reaction with morpholine. *Anal Chem* 1955, 27, 1464.
24. Carlson, D.; Nie, L.; Narayan, R.; Dubois, P. *J Appl Polym Sci* 1999, 72, 477.
25. Flory, P. J. *Principles of Polymer Chemistry*; Cornell University Press: Ithaca, 1953.
26. Catiker, E.; Gumusderelioglu, M.; Guner, A. *Polym Int* 2000, 49, 728.
27. Peesan, M.; Supaphol, P.; Rujiravanit, R. *Carbohydr Polym* 2005, 60, 343.
28. Rafler, G.; Dahlmann, J.; Wiener, K. *Acta Polym* 1990, 41, 328.
29. Avella, M.; Errico, M. E.; Immirzi, B.; Malinconico, M.; Martuscelli, E.; Paolillo, L.; Falcigno, L. *Angew Makromol Chem* 1997, 246, 49.
30. Martins, M. A.; Kiyohara, P. K.; Joekes, I. *J Appl Polym Sci* 2004, 94, 2333.
31. Hill, C. A. S.; Abdul Khalil, H. P. S. *J Appl Polym Sci* 2000, 78, 1685.
32. Mani, R.; Bhattacharya, M.; Tang, J. *J Polym Sci Part A: Polym Chem* 1999, 37, 1693.
33. Avella, M.; Errico, M. E.; Rimedio, R.; Sadocco, P. *J Appl Polym Sci* 2002, 83, 1432.
34. Chen, C.; Zhou, X.; Zhuang, Y.; Dong, L. *J Polym Sci Part B: Polym Phys* 2005, 43, 35.
35. Chen, C.; Peng, S.; Fei, B.; Zhuang, Y.; Dong, L.; Feng, Z.; Chen, S.; Xia, H. *J Appl Polym Sci* 2003, 88, 659.
36. Assan, M. L.; Rowell, R. M.; Fadl, N. A.; Yacoub, S. F.; Christensen, A. W. *J Appl Polym Sci* 2000, 76, 561.
37. Montaudo, G.; Puglisi, C.; Samperi, F. *J Polym Sci Part A: Polym Chem* 1994, 32, 15.
38. Montaudo, G.; Puglisi, C.; Samperi, F. *Macromolecules* 1998, 31, 650.
39. Porter, R. S.; Wang, L.-H. *Polymer* 1992, 33, 2019.
40. Hamilton, D. G.; Gallucci, R. R. *J Appl Polym Sci* 1993, 48, 2249.
41. Miley, D. M.; Runt, J. *Polymer* 1992, 33, 4643.
42. Puglia, D.; Tomassucci, A.; Kenny, J. M. *Polym Adv Technol* 2003, 14, 749.
43. Avella, M.; Dell'Erba, R.; Martuscelli, E.; Partch, R. *J Polym Mater* 2000, 17, 445.
44. Avella, M.; Dell'Erba, R.; Focher, B.; Marzetti, A.; Martuscelli, E. *Angew Makromol Chem* 1995, 233, 149.
45. Kubat, J.; Rigdahl, M.; Welander, M. *J Appl Polym Sci* 1990, 39, 1527.